

Measurement of Branching Fraction and Direct CP Asymmetry in $B^0 \rightarrow \rho^0 \pi^0$ Decays

J. Dragic,⁶ K. Abe,⁶ K. Abe,⁴¹ I. Adachi,⁶ H. Aihara,⁴³ D. Anipko,¹ Y. Asano,⁴⁷ T. Aushev,¹⁰ S. Bahinipati,⁴ A. M. Bakich,³⁸ V. Balagura,¹⁰ M. Barbero,⁵ A. Bay,¹⁵ I. Bedny,¹ U. Bitenc,¹¹ I. Bizjak,¹¹ S. Blyth,²¹ A. Bondar,¹ A. Bozek,²⁴ M. Bračko,^{17,11} J. Brodzicka,²⁴ T. E. Browder,⁵ M.-C. Chang,⁴² P. Chang,²³ Y. Chao,²³ A. Chen,²¹ W. T. Chen,²¹ B. G. Cheon,³ R. Chistov,¹⁰ Y. Choi,³⁷ Y. K. Choi,³⁷ A. Chuvikov,³¹ S. Cole,³⁸ J. Dalseno,¹⁸ M. Danilov,¹⁰ M. Dash,⁴⁸ A. Drutskoy,⁴ S. Eidelman,¹ N. Gabyshev,¹ A. Garmash,³¹ T. Gershon,⁶ A. Go,²¹ G. Gokhroo,³⁹ B. Golob,^{16,11} A. Gorišek,¹¹ H. C. Ha,¹³ J. Haba,⁶ T. Hara,²⁸ N. C. Hastings,⁴³ K. Hayasaka,¹⁹ H. Hayashii,²⁰ M. Hazumi,⁶ L. Hinz,¹⁵ Y. Hoshi,⁴¹ S. Hou,²¹ W.-S. Hou,²³ Y. B. Hsiung,²³ T. Iijima,¹⁹ K. Ikado,¹⁹ K. Inami,¹⁹ A. Ishikawa,⁶ H. Ishino,⁴⁴ R. Itoh,⁶ M. Iwasaki,⁴³ Y. Iwasaki,⁶ C. Jacoby,¹⁵ J. H. Kang,⁴⁹ P. Kapusta,²⁴ N. Katayama,⁶ H. Kawai,² T. Kawasaki,²⁵ H. Kichimi,⁶ H. J. Kim,¹⁴ S. K. Kim,³⁵ S. M. Kim,³⁷ K. Kinoshita,⁴ S. Korpar,^{17,11} P. Križan,^{16,11} P. Krokovny,¹ R. Kulasiri,⁴ C. C. Kuo,²¹ A. Kusaka,⁴³ A. Kuzmin,¹ Y.-J. Kwon,⁴⁹ G. Leder,⁸ J. Lee,³⁵ T. Lesiak,²⁴ J. Li,³⁴ A. Limosani,⁶ S.-W. Lin,²³ D. Liventsev,¹⁰ J. MacNaughton,⁸ F. Mandl,⁸ D. Marlow,³¹ T. Matsumoto,⁴⁵ Y. Mikami,⁴² W. Mitaroff,⁸ K. Miyabayashi,²⁰ H. Miyake,²⁸ H. Miyata,²⁵ Y. Miyazaki,¹⁹ R. Mizuk,¹⁰ D. Mohapatra,⁴⁸ T. Mori,⁴⁴ M. Nakao,⁶ Z. Natkaniec,²⁴ S. Nishida,⁶ O. Nitoh,⁴⁶ T. Nozaki,⁶ S. Ogawa,⁴⁰ T. Ohshima,¹⁹ T. Okabe,¹⁹ S. Okuno,¹² S. L. Olsen,⁵ W. Ostrowicz,²⁴ H. Ozaki,⁶ C. W. Park,³⁷ H. Park,¹⁴ R. Pestotnik,¹¹ L. E. Piilonen,⁴⁸ M. Rozanska,²⁴ Y. Sakai,⁶ T. R. Sarangi,⁶ N. Sato,¹⁹ N. Satoyama,³⁶ T. Schietinger,¹⁵ O. Schneider,¹⁵ J. Schümann,²³ C. Schwanda,⁸ A. J. Schwartz,⁴ R. Seidl,³² K. Senyo,¹⁹ M. E. Sevier,¹⁸ M. Shapkin,⁹ H. Shibuya,⁴⁰ B. Shwartz,¹ J. B. Singh,²⁹ A. Sokolov,⁹ A. Somov,⁴ N. Soni,²⁹ R. Stamen,⁶ S. Stanič,²⁶ M. Starič,¹¹ K. Sumisawa,²⁸ T. Sumiyoshi,⁴⁵ S. Suzuki,³³ O. Tajima,⁶ F. Takasaki,⁶ K. Tamai,⁶ N. Tamura,²⁵ M. Tanaka,⁶ G. N. Taylor,¹⁸ Y. Teramoto,²⁷ X. C. Tian,³⁰ K. Trabelsi,⁵ T. Tsuboyama,⁶ T. Tsukamoto,⁶ S. Uehara,⁶ T. Uglov,¹⁰ Y. Unno,⁶ S. Uno,⁶ P. Urquijo,¹⁸ Y. Ushiroda,⁶ Y. Usov,¹ G. Varner,⁵ S. Villa,¹⁵ C. C. Wang,²³ C. H. Wang,²² M.-Z. Wang,²³ Y. Watanabe,⁴⁴ J. Wicht,¹⁵ E. Won,¹³ Q. L. Xie,⁷ B. D. Yabsley,³⁸ A. Yamaguchi,⁴² M. Yamauchi,⁶ J. Ying,³⁰ C. C. Zhang,⁷ J. Zhang,⁶ L. M. Zhang,³⁴ Z. P. Zhang,³⁴ V. Zhilich,¹ and D. Zürcher¹⁵

(The Belle Collaboration)

¹Budker Institute of Nuclear Physics, Novosibirsk

²Chiba University, Chiba

³Chonnam National University, Kwangju

⁴University of Cincinnati, Cincinnati, Ohio 45221

⁵University of Hawaii, Honolulu, Hawaii 96822

⁶High Energy Accelerator Research Organization (KEK), Tsukuba

⁷Institute of High Energy Physics, Chinese Academy of Sciences, Beijing

⁸Institute of High Energy Physics, Vienna

⁹Institute of High Energy Physics, Protvino

¹⁰Institute for Theoretical and Experimental Physics, Moscow

¹¹J. Stefan Institute, Ljubljana

¹²Kanagawa University, Yokohama

¹³Korea University, Seoul

¹⁴Kyungpook National University, Taegu

¹⁵Swiss Federal Institute of Technology of Lausanne, EPFL, Lausanne

¹⁶University of Ljubljana, Ljubljana

¹⁷University of Maribor, Maribor

¹⁸University of Melbourne, Victoria

¹⁹Nagoya University, Nagoya

²⁰Nara Women's University, Nara

²¹National Central University, Chung-li

²²National United University, Miao Li

²³Department of Physics, National Taiwan University, Taipei

²⁴H. Niewodniczanski Institute of Nuclear Physics, Krakow

²⁵Niigata University, Niigata

²⁶Nova Gorica Polytechnic, Nova Gorica

²⁷Osaka City University, Osaka

²⁸*Osaka University, Osaka*
²⁹*Panjab University, Chandigarh*
³⁰*Peking University, Beijing*
³¹*Princeton University, Princeton, New Jersey 08544*
³²*RIKEN BNL Research Center, Upton, New York 11973*
³³*Saga University, Saga*
³⁴*University of Science and Technology of China, Hefei*
³⁵*Seoul National University, Seoul*
³⁶*Shinshu University, Nagano*
³⁷*Sungkyunkwan University, Suwon*
³⁸*University of Sydney, Sydney NSW*
³⁹*Tata Institute of Fundamental Research, Bombay*
⁴⁰*Toho University, Funabashi*
⁴¹*Tohoku Gakuin University, Tagajo*
⁴²*Tohoku University, Sendai*
⁴³*Department of Physics, University of Tokyo, Tokyo*
⁴⁴*Tokyo Institute of Technology, Tokyo*
⁴⁵*Tokyo Metropolitan University, Tokyo*
⁴⁶*Tokyo University of Agriculture and Technology, Tokyo*
⁴⁷*University of Tsukuba, Tsukuba*
⁴⁸*Virginia Polytechnic Institute and State University, Blacksburg, Virginia 24061*
⁴⁹*Yonsei University, Seoul*

We report a measurement of the branching fraction of the decay $B^0 \rightarrow \rho^0 \pi^0$, using 386×10^6 $B\bar{B}$ pairs collected at the $\Upsilon(4S)$ resonance with the Belle detector at the KEKB asymmetric-energy e^+e^- collider. We detect 51^{+14}_{-13} signal events with a significance of 4.2 standard deviations, including systematic uncertainties, and measure the branching fraction to be $\mathcal{B}(B^0 \rightarrow \rho^0 \pi^0) = (3.12^{+0.88}_{-0.82}(\text{stat}) \pm 0.33(\text{syst})^{+0.50}_{-0.68}(\text{model})) \times 10^{-6}$. We also perform the first measurement of direct CP violating asymmetry in this mode.

PACS numbers: 11.30.Er, 12.15.Hh, 13.25.Hw, 14.40.Nd

Tests of the Kobayashi-Maskawa model [1] for CP violation are ongoing. In particular, B -factories are directing focus towards measurements of the lesser known angles of the Cabibbo-Kobayashi-Maskawa (CKM) triangle, ϕ_2 and ϕ_3 . Measurements of ϕ_2 typically rely on time-dependent CP -violation studies of B meson decays to $\pi^+\pi^-$, $\rho^\pm\pi^\mp$ and $\rho^+\rho^-$ [2, 3], since the leading tree amplitudes for these processes involve the relevant CKM phases. However, penguin amplitudes may also contribute significantly in these decays and — via introducing additional unknown phases — greatly impair ϕ_2 constraints from the time-dependent measurements. In such cases, isospin analyses can be employed to separate the tree-level process from penguin contamination [4].

Measurements of ϕ_2 from the $\rho\pi$ system rely on knowledge of the $B^0 \rightarrow \rho^0 \pi^0$ branching fraction [4, 5]. Since the tree amplitude of $B^0 \rightarrow \rho^0 \pi^0$ decay is color suppressed, the decay rate is sensitive to the penguin amplitude contribution. Thus, the $\rho^0 \pi^0$ branching fraction plays a critical role in constraining the ϕ_2 uncertainty due to penguin pollution from time-dependent $B^0 \rightarrow \rho^\pm\pi^\mp$ measurements [3, 4]. Furthermore, measurement of ϕ_2 from the full $B \rightarrow \rho\pi$ isospin analysis requires the $\rho^0 \pi^0$ branching fraction along with its CP asymmetry. Since the branching fractions and CP asymmetries of all the other $\rho\pi$ final states have been measured [6], $\rho^0 \pi^0$ is the only channel that remains to complete the isospin pen-

tagons. A simplification, whereby the pentagons collapse into quadrangles, is also possible if the $\rho^0 \pi^0$ amplitude is sufficiently small.

An alternative technique to measure ϕ_2 from the $\rho\pi$ system, even if penguin contamination is large, is a time-dependent amplitude analysis of $B^0 \rightarrow \pi^+\pi^-\pi^0$ [5]. Here, the interferences between $\rho^+\pi^-$, $\rho^0\pi^0$ and $\rho^-\pi^+$ contributions to the $\pi^+\pi^-\pi^0$ final state provide the critical information on the unknown phases introduced by penguin amplitudes. Recently, the first time-dependent studies of the $\pi^+\pi^-\pi^0$ Dalitz plot have been performed [7]. In these studies, a simplification is made with the assumption that the $\rho^0\pi^0$ contribution is small. A more complex time-dependent Dalitz analysis is required if this is not the case.

The Belle Collaboration reported first evidence of the $B^0 \rightarrow \rho^0 \pi^0$ decay [8] with a branching fraction larger than most predictions [9], and a central value above the 90% confidence-level upper limit set by the BaBar Collaboration [10]. In this paper, we report an improved measurement of the $B^0 \rightarrow \rho^0 \pi^0$ branching fraction [11], using 2.5 times more data, and perform a first direct CP violation search in this mode. The results are consistent with and supersede those reported in our previous publication. The analysis is based on $(385.8 \pm 4.8) \times 10^6$ $B\bar{B}$ pairs, collected with the Belle detector at the KEKB asymmetric-energy e^+e^- collider [12] that operates at the

$\Upsilon(4S)$ resonance. The production rates of B^+B^- and $B^0\overline{B}^0$ pairs are assumed to be equal.

The Belle detector [13, 14] is a large-solid-angle magnetic spectrometer that consists of a silicon vertex detector, a 50-layer central drift chamber (CDC), an array of aerogel threshold Cherenkov counters (ACC), a barrel-like arrangement of time-of-flight scintillation counters (TOF), and an electromagnetic calorimeter comprised of CsI(Tl) crystals (ECL) located inside a superconducting solenoid coil that provides a 1.5 T magnetic field. An iron flux-return located outside of the coil is instrumented to detect K_L^0 mesons and to identify muons.

The B reconstruction procedure is identical to our previously published analysis [8]. Charged tracks are required to originate from the interaction point and have transverse momenta greater than 100 MeV/ c . Pions are identified by combining information from the ACC, TOF and the CDC dE/dx measurements. We further reject tracks that are consistent with an electron hypothesis. Pairs of photons with invariant masses in the range $0.115 \text{ GeV}/c^2 < m_{\gamma\gamma} < 0.154 \text{ GeV}/c^2$ are used to form the π^0 mesons. The photon energy in the laboratory frame is required to be greater than 50 (100) MeV in the barrel (endcap) region of the ECL. The π^0 candidates are required to have transverse momenta greater than 100 MeV/ c in the laboratory frame and a loose requirement is made on $\chi^2_{\pi^0}$, the goodness of fit of a π^0 mass-constrained fit of the two photons. We also veto possible contributions to $\pi^+\pi^-\pi^0$ from charmed ($b \rightarrow c$) decays: $B^0 \rightarrow D^-\pi^+, \overline{D}^0\pi^0$ and $J/\psi\pi^0$.

Signal B candidates are identified with two kinematic variables: the beam-energy constrained mass $M_{bc} \equiv \sqrt{E_{\text{beam}}^2/c^4 - p_B^2/c^2}$ and the energy difference $\Delta E \equiv E_B - E_{\text{beam}}$. Here, E_B (p_B) is the reconstructed energy (momentum) of the B candidate, and E_{beam} is the beam energy, all expressed in the centre-of-mass (CM) frame. We consider candidate events in the region $-0.2 \text{ GeV} < \Delta E < 0.4 \text{ GeV}$ and $M_{bc} > 5.23 \text{ GeV}/c^2$; and define signal regions in ΔE and M_{bc} as $-0.135 \text{ GeV} < \Delta E < 0.082 \text{ GeV}$ and $5.269 \text{ GeV}/c^2 < M_{bc} < 5.290 \text{ GeV}/c^2$. To select $\rho^0\pi^0$ from the $\pi^+\pi^-\pi^0$ candidates, we require the $\pi^+\pi^-$ invariant mass to be in the range $0.5 \text{ GeV}/c^2 < m_{\pi^+\pi^-} < 1.1 \text{ GeV}/c^2$ and the ρ^0 helicity angle to satisfy $|\cos\theta_{\text{hel}}^\rho| > 0.5$, where θ_{hel}^ρ is defined as the angle between the negative pion direction and the opposite of the B direction in the ρ rest frame. We explicitly veto contributions from $B^0 \rightarrow \rho^\pm\pi^\mp$ by the requirement $m_{\pi^\pm\pi^0} > 1.1 \text{ GeV}/c^2$. This requirement also vetoes the region of the Dalitz plot where the interference between $\rho^0\pi^0$ and $\rho^\pm\pi^\mp$ is strongest. After all selection requirements, 11% of events have more than one candidate. Among those candidates the one with the smallest $\chi^2_{\text{vtx}}/ndf + \chi^2_{\pi^0}/ndf$ is selected, where χ^2_{vtx} is the goodness of fit of a vertex-constrained fit of $\pi^+\pi^-$.

The dominant background originates from continuum $e^+e^- \rightarrow q\bar{q}$ ($q = u, d, s, c$) production. To separate the

jet-like $q\bar{q}$ events, we use event shape variables: five modified Fox-Wolfram moments [15], combined into a Fisher discriminant. We further combine the cosine of the B meson flight direction in the CM system with the output of the Fisher discriminant into a signal/background likelihood variable, $\mathcal{L}_{s/b}$, and define the likelihood ratio $\mathcal{R} = \mathcal{L}_s / (\mathcal{L}_s + \mathcal{L}_b)$. Additional discrimination against continuum is achieved through use of the b -flavour tagging algorithm [16]. We use the parameter r , with values between 0 and 1, as a measure of the confidence that the remaining particles in the event (other than $\pi^+\pi^-\pi^0$) originated from a flavour specific B meson decay and — as a corollary — not from a continuum process.

We use an iterative procedure to find the optimal contiguous area in $r\mathcal{R}$ space by maximising $N_s/\sqrt{N_s + N_b}$, where N_s (N_b) is the expected number of signal (background) events in the ΔE and M_{bc} signal regions. Here, the optimisation procedure assumes a branching fraction for $B^0 \rightarrow \rho^0\pi^0$ of 3.3×10^{-6} [17]. Anticipating the use of r for its primary purpose of flavour tagging in CP asymmetry fits, the borders of the contiguous area were constrained to match the six r bins employed in previous analyses. The result of the optimisation procedure is that we select events within the region shown in Fig. 1(a). We find 1397 candidates remain in the data.

We obtain the signal yield using an extended unbinned maximum-likelihood fit to the ΔE - M_{bc} distribution of the selected candidate events. The likelihood function is defined as

$$\mathcal{L} = \exp \left(- \sum_{j,l} N_{j,l} \right) \prod_i \left(\sum_{j,l} N_{j,l} \mathcal{P}_j^i \right). \quad (1)$$

Here, the index i is the event identifier; l distinguishes events in various r bins; and j runs over all six components included in the fitting function — one for the signal, and the others for continuum, $b \rightarrow c$ combinatorial, and the charmless B backgrounds: $B^+ \rightarrow \rho^+\rho^0$, $B^+ \rightarrow \rho^+\pi^0$ and $B^+ \rightarrow \pi^+\pi^0$. $N_{j,l}$ represents the number of events, and $\mathcal{P}_j^i = P_j(M_{bc}^i, \Delta E^i)$ are two-dimensional probability density functions (PDFs).

The PDFs for signal, $b \rightarrow c$ and charmless B backgrounds are taken from smoothed two-dimensional histograms obtained from Monte Carlo (MC) simulations. For the $B^+ \rightarrow \rho^+\rho^0$ channel, we assume a 100% longitudinally polarised decay [18]. Small corrections to MC peak positions and widths are applied to the signal PDF. These factors are derived from control samples of reconstructed decays $B^0 \rightarrow D^{*-}\rho^+$ ($D^{*-} \rightarrow \overline{D}^0\pi^-$, $\overline{D}^0 \rightarrow K^+\pi^-$; $\rho^+ \rightarrow \pi^+\pi^0$) and $B^+ \rightarrow \overline{D}^0\rho^+$ ($\overline{D}^0 \rightarrow K^+\pi^-$; $\rho^+ \rightarrow \pi^+\pi^0$), in which we require that the π^0 momentum be greater than 1.8 GeV/ c in order to mimic the high momentum π^0 in our signal. The two-dimensional PDF for the continuum background is described as the product of a first-order polynomial in ΔE and an ARGUS function [19] in M_{bc} . All of the shape parameters describing

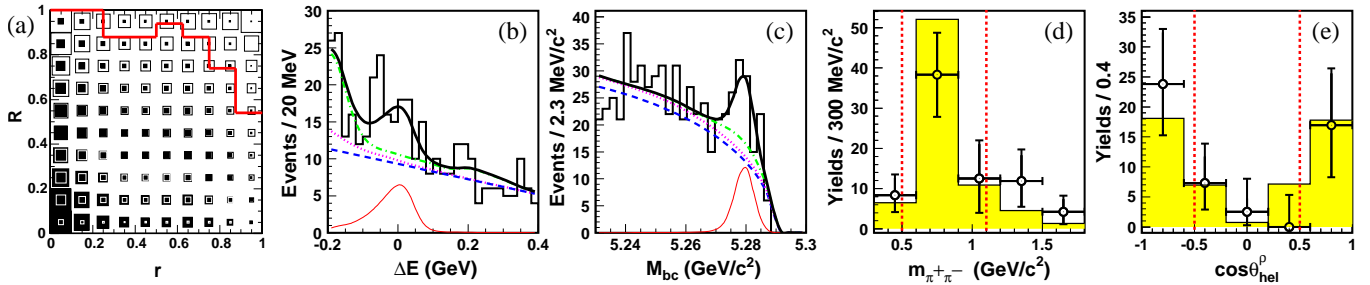


FIG. 1: (a) Distribution of signal (continuum) events in r - \mathcal{R} space shown with open (shaded) proportional boxes; the marked region (top-right) indicates the area selected. (b) (c) Distribution of $\Delta E(M_{bc})$ in the signal region of $M_{bc}(\Delta E)$. Projection of the fit result is shown as the thick solid curve; the thin solid line represents the signal component; the dashed, dotted and dash-dotted curves represent, respectively, the cumulative background components from continuum processes, $b \rightarrow c$ decays, and charmless B backgrounds. (d), (e) Distributions of fit yields in $m_{\pi^+\pi^-}$ and $\cos\theta_{\text{hel}}^\rho$ variables for $\rho^0\pi^0$ candidate events. Points with error bars represent data fit results, and the histograms show signal MC expectation; the selection requirements described in the text are shown as dashed lines.

the continuum background are free parameters in the fit. The normalisations of $B^+ \rightarrow \rho^+\pi^0$ (21.7 ± 4.4 events) and $B^+ \rightarrow \pi^+\pi^0$ (21.0 ± 5.5 events) are fixed in the fit according to previous measurements [6, 20], and that of $b \rightarrow c$ background (62 ± 62 events) according to MC expectation (assigning a conservative error); the normalisations of all other components are allowed to float.

The fit result is shown in Fig. 1(b) and (c). The signal yield is found to be $50.9^{+14.3}_{-13.4}$ with 4.5σ significance. The significance is defined as $\sqrt{-2 \ln(\mathcal{L}_0/\mathcal{L}_{\text{max}})}$, where \mathcal{L}_{max} (\mathcal{L}_0) denotes the likelihood with the signal yield at its nominal value (fixed to zero). The contribution from $B^+ \rightarrow \rho^+\rho^0$ decays (which peaks in the low ΔE region) is obtained from the fit as $43.1^{+13.2}_{-12.1}$ events; this value is consistent with the MC expectation ($33.9^{+8.1}_{-9.8}$ events) based on our branching fraction measurement of $B^+ \rightarrow \rho^+\rho^0$ [18]. A possible contribution from $B \rightarrow \omega(\pi^+\pi^-\pi^0)\pi^0$ decays is also accounted for by floating the $B^+ \rightarrow \rho^+\rho^0$ PDF, since the two decays have similar distributions in ΔE and M_{bc} . To verify that the signal candidates originate from $B^0 \rightarrow \rho^0\pi^0$ decays, we change the criteria on $m_{\pi^+\pi^-}$ and $\cos\theta_{\text{hel}}^\rho$ in turn, and repeat fits to the ΔE - M_{bc} distribution. The yields obtained in each $m_{\pi^+\pi^-}$ and $\cos\theta_{\text{hel}}^\rho$ bin are shown in Fig. 1(d) and (e).

The $\cos\theta_{\text{hel}}^\rho$ distribution is used to limit contributions from $B^0 \rightarrow \sigma\pi^0$, $f_0(980)\pi^0$, $\eta'\pi^0$, $K_S\pi^0$ and $\pi^+\pi^-\pi^0$ (nonresonant), which are expected to be flat in this variable. We perform a χ^2 fit including components for pseudoscalar \rightarrow pseudoscalar vector ($PV \sim \cos^2\theta_{\text{hel}}^\rho$), and pseudoscalar \rightarrow pseudoscalar scalar ($PS \sim \text{flat}$) decays, for which the shapes are obtained from our $\rho^0\pi^0$ signal MC, and a sample of $\sigma\pi^0$ MC [21], respectively. We also include a linear term to allow for possible interference. We find that the PS level is consistent with zero; taking its uncertainty into account, we assign a model error of $^{+0.0}_{-15.0}\%$ to the PV component. The $m_{\pi^+\pi^-}$ distribution is consistent with the expectation from $B^0 \rightarrow \rho^0\pi^0$

production.

To extract the branching fraction, we determine the reconstruction efficiency, $(4.99 \pm 0.03)\%$, from MC and correct for small differences between data and MC in the pion identification and continuum suppression requirements. The correction factor due to charged pion identification (0.872) is obtained in bins of track momentum and polar angle from an inclusive D^* control sample ($D^{*-} \rightarrow \bar{D}^0\pi^-$, $\bar{D}^0 \rightarrow K^+\pi^-$). The corresponding systematic error is $\pm 3.1\%$. For the continuum suppression requirement on r and \mathcal{R} , we use the control sample $B^0 \rightarrow D^-\rho^+$ ($D^- \rightarrow K^+\pi^-\pi^-$; $\rho^+ \rightarrow \pi^+\pi^0$) to obtain an efficiency correction factor of 0.972 and a corresponding systematic error of $\pm 6.0\%$.

We calculate additional systematic errors from the following sources: PDF shapes by varying parameters by $\pm 1\sigma$ ($^{+0.9}_{-2.0}\%$); π^0 reconstruction efficiency by comparing the yields of $\eta \rightarrow \pi^0\pi^0\pi^0$ and $\eta \rightarrow \gamma\gamma$ between data and MC ($\pm 4.0\%$); track finding efficiency from a study of partially reconstructed D^* decays ($\pm 2.4\%$); and data-MC efficiency differences due to the $\Delta E > -0.2$ GeV requirement ($\pm 2.0\%$). We repeat the fit after changing the normalisation of the fixed background components according to the given errors and obtain a systematic error of $^{+2.0}_{-1.8}\%$. Using a large MC sample, the total systematic error from possible charmless B decays not otherwise included, $B^0 \rightarrow K^{*0}\pi^0$ (5.4%), $B^+ \rightarrow K^{*+}\pi^0$ (1.5%) and $B^0 \rightarrow K^+\rho^-$ (0.5%), is $\pm 5.6\%$.

When the normalisations of all the backgrounds fixed in the fit are simultaneously increased by 1σ , the statistical significance decreases from 4.5σ to 4.2σ ; we interpret the latter value as the significance of our result. Finally, we estimate the uncertainty due to possible interference with $B^0 \rightarrow \rho^\pm\pi^\mp$ by varying the $m_{\pi^\pm\pi^0}$ veto requirement from $m_{\pi^\pm\pi^0} > 0$ MeV/ c^2 (no veto) to $m_{\pi^\pm\pi^0} > 1.7$ GeV/ c^2 . We find the largest change in the result to be within $\pm 16\%$, and we include this value in the model error, so that the obtained $B^0 \rightarrow \rho^0\pi^0$ branching

fraction is

$$\mathcal{B} = (3.12^{+0.88}_{-0.82}(\text{stat}) \pm 0.33(\text{syst})^{+0.50}_{-0.68}(\text{model})) \times 10^{-6}.$$

Having observed a significant $B^0 \rightarrow \rho^0 \pi^0$ signal, we utilize the B^0/\bar{B}^0 separation provided by the flavour tagging to measure the CP asymmetry. For this purpose we replace \mathcal{P}_j^i of Eq. (1) with the expression

$$\mathcal{P}_{j,l}^i = \frac{1}{2} \left[1 + q^i \cdot (\mathcal{A}'_{CP})_{j,l} \right] P_j(M_{bc}^i, \Delta E^i), \quad (2)$$

in which the indices keep the same meaning. In this equation, q represents the b -flavour charge [$q = +1(-1)$ when the tagging B meson is a B^0 (\bar{B}^0)] and \mathcal{A}'_{CP} denotes the effective charge asymmetry, such that $(\mathcal{A}'_{CP})_{j,l} = (\mathcal{A}_{CP})_j(1 - 2\chi_d)(1 - 2w_l)$. Here, $(\mathcal{A}_{CP})_j$ are the charge asymmetries for the signal and the background components. Further, $\chi_d = 0.182 \pm 0.015$ [22] is the time-integrated mixing parameter and w_l is the wrong-tag fraction. For continuum background, χ_d and w_l are set to zero. The data is divided into the six r -bins, and the r -dependent wrong-tag fractions, w_l ($l = 1, \dots, 6$), are determined using a high statistics sample of self-tagged $B^0 \rightarrow D^{(*)-} \pi^+, D^{*-} \rho^+$ and $D^{*-} \ell^+ \nu$ events [16].

The total number of signal, continuum background and $\rho^+ \rho^0$ events are free parameters in the fit, and the remaining background components (from $b \rightarrow c$, $\rho^+ \pi^0$ and $\pi^+ \pi^0$ decays) are fixed. Also, the relative fractions for the signal and continuum background components in different r bins are allowed to float in the fit; for the $b \rightarrow c$ and charmless B decay backgrounds, they are fixed. The only free \mathcal{A}_{CP} parameter in the nominal fit is that of our signal; the others are fixed to be zero (for continuum and $b \rightarrow c$) or at their previously measured values (for charmless B backgrounds) [20]. We measure the direct CP asymmetry in $B^0 \rightarrow \rho^0 \pi^0$ decays to be

$$\mathcal{A}_{CP} = -0.53^{+0.67}_{-0.84}(\text{stat})^{+0.10}_{-0.15}(\text{syst}).$$

The impact of background asymmetry ($^{+0.058}_{-0.127}$) is the largest contribution to the systematic error; it is estimated by releasing, in turn, all of the background \mathcal{A}_{CP} parameters (limiting them within $\pm 1\sigma$ range of their measured values for the charmless B decays), and summing in quadrature the differences obtained from the central \mathcal{A}_{CP} value. A similar sum gives $^{+0.059}_{-0.057}$ as the systematic uncertainty obtained by varying all other fixed parameters in the fit, including χ_d and w_l values, by $\pm 1\sigma$. Finally a systematic error of ± 0.058 is obtained as a result of a null asymmetry test, when the same analysis procedure is applied to the $B^0 \rightarrow D^- \rho^+$ ($D^- \rightarrow K^+ \pi^- \pi^-$; $\rho^+ \rightarrow \pi^+ \pi^0$) control sample. To illustrate the asymmetry, we show the results separately for $\rho^0 \pi^0$ candidate events tagged as $q = +1$ and $q = -1$ in Fig. 2.

In summary, using $386 \times 10^6 B\bar{B}$ pairs, we confirm evidence of $B^0 \rightarrow \rho^0 \pi^0$ decays with a branching fraction

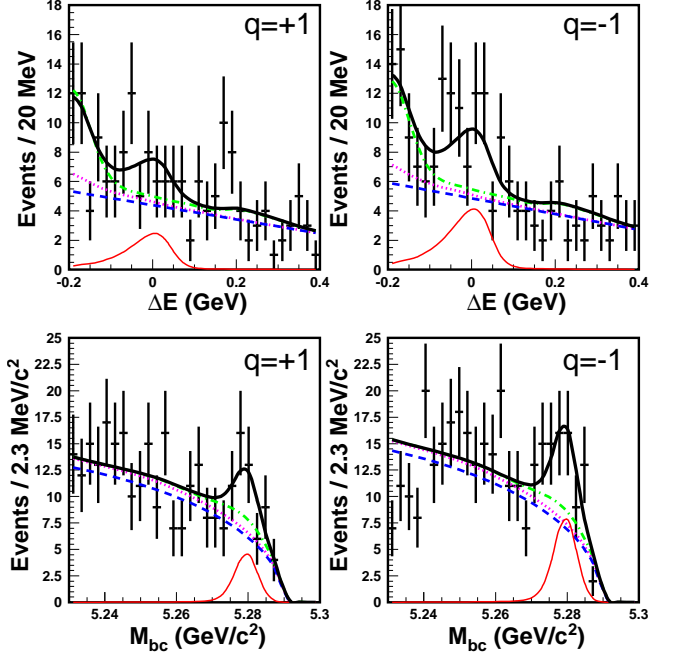


FIG. 2: ΔE and M_{bc} distributions (with projections of the fit results) shown separately for events tagged as $q = +1$ (left) and $q = -1$ (right).

higher than most theoretical predictions [9]. The central value remains only slightly above the 90% confidence-level upper limit set by the BaBar Collaboration [10], and is in agreement with the upper limit set by the CLEO Collaboration [6]. Our measurement is consistent with, and supersedes, our previous result [8]. We have also performed a first measurement of direct CP violation in the $B^0 \rightarrow \rho^0 \pi^0$ mode and find no statistically significant asymmetry.

The large $\rho^0 \pi^0$ branching fraction suggest that one can only impose a loose constraint on penguin uncertainty in the determination of ϕ_2 from time-dependent $B^0 \rightarrow \rho^\pm \pi^\mp$ measurements. It also implies that a useful measurement of ϕ_2 from the full $\rho\pi$ isospin analysis may be impractical even with super B -factory like luminosities [23]. Therefore, we can expect that the best measurements of ϕ_2 from the $\rho\pi$ system will come from the full time-dependent amplitude analysis of $B^0 \rightarrow \pi^+ \pi^- \pi^0$.

We thank the KEKB group for excellent operation of the accelerator, the KEK cryogenics group for efficient solenoid operations, and the KEK computer group and the NII for valuable computing and Super-SINET network support. We acknowledge support from MEXT and JSPS (Japan); ARC and DEST (Australia); NSFC and KIP of CAS (contract No. 10575109 and IHEP-U-503, China); DST (India); the BK21 program of MOEHRD, and the CHEP SRC and BR (grant No. R01-2005-000-10089-0) programs of KOSEF (Korea); KBN (contract No. 2P03B 01324, Poland); MIST (Russia); MHEST (Slovenia); SNSF (Switzerland); NSC and MOE (Tai-

wan); and DOE (USA).

[1] M. Kobayashi and T. Maskawa, *Prog. Theor. Phys.* **49**, 652 (1973).

[2] K. Abe *et al.* (Belle Collab.), *Phys. Rev. Lett.* **95**, 101801 (2005); B. Aubert *et al.* (BaBar Collab.), *Phys. Rev. Lett.* **95**, 151803 (2005); A. Somov *et al.* (Belle Collab.), [hep-ex/0601024](#), to appear in *Phys. Rev. Lett.*; B. Aubert *et al.* (BaBar Collab.), *Phys. Rev. Lett.* **95**, 041805 (2005).

[3] C. C. Wang *et al.* (Belle Collab.), *Phys. Rev. Lett.* **94**, 121801 (2005).

[4] M. Gronau and D. London, *Phys. Rev. Lett.* **65**, 3381 (1990); H. J. Lipkin, Y. Nir, H. R. Quinn and A. E. Snyder, *Phys. Rev. D* **44**, 1454 (1991); Y. Grossman and H. R. Quinn, *Phys. Rev. D* **58**, 017504 (1998). M. Gronau, D. London, N. Sinha and R. Sinha, *Phys. Lett. B* **514**, 315 (2001).

[5] A. E. Snyder and H. R. Quinn, *Phys. Rev. D* **48**, 2139 (1993).

[6] A. Gordon *et al.* (Belle Collab.), *Phys. Lett. B* **542**, 183 (2002); B. Aubert *et al.* (BaBar Collab.), *Phys. Rev. Lett.* **91**, 201802 (2003); J. Zhang *et al.* (Belle Collab.), *Phys. Rev. Lett.* **94**, 031801 (2005); C.-P. Jessop *et al.* (CLEO Collab.), *Phys. Rev. Lett.* **85**, 2881 (2000).

[7] B. Aubert *et al.* (BaBar Collab.), [hep-ex/0408099](#), submitted to the ICHEP 04 conference.

[8] J. Dragic *et al.* (Belle Collab.), *Phys. Rev. Lett.* **93**, 131802 (2004).

[9] C.-W. Chiang, M. Gronau, Z. Luo, J. L. Rosner and D. A. Suprun, *Phys. Rev. D* **69**, 034001 (2004); M. Beneke and M. Neubert, *Nucl. Phys. B* **675**, 333 (2003).

[10] B. Aubert *et al.* (BaBar Collab.), *Phys. Rev. Lett.* **93**, 051802 (2004).

[11] Throughout the paper, the inclusion of the charge conjugate mode decay is implied unless otherwise stated.

[12] S. Kurokawa and E. Kikutani, *Nucl. Instr. and Meth. A* **499**, 1 (2003), and other papers included in this volume.

[13] A. Abashian *et al.* (Belle Collab.), *Nucl. Instr. and Meth. A* **479**, 117 (2002).

[14] Y. Ushiroda (Belle SVD2 Group), *Nucl. Instr. and Meth. A* **511**, 6 (2003).

[15] G. Fox and S. Wolfram, *Phys. Rev. Lett.* **41**, 1581 (1978).

[16] H. Kakuno *et al.*, *Nucl. Instr. and Meth. A* **533**, 516 (2004).

[17] The number is the average of central values reported in references [8, 10].

[18] J. Zhang *et al.* (Belle Collab.), *Phys. Rev. Lett.* **91**, 221801 (2003).

[19] H. Albrecht *et al.* (ARGUS Collab.), *Phys. Lett. B* **241**, 278 (1990).

[20] S. Eidelman *et al.* (Particle Data Group), *Phys. Lett. B* **592**, 1 (2004) and 2005 partial update for edition 2006.

[21] We model the σ particle with a mass of $478 \text{ MeV}/c^2$ and a width of $324 \text{ MeV}/c^2$, based on E. M. Aitala *et al.* (E791 Collab.), *Phys. Rev. Lett.* **86**, 770 (2001).

[22] Heavy Flavor Averaging Group (HFAG), “Averages of b-hadron Properties as of Winter 2005”, [hep-ex/0505100](#).

[23] J. Stark, *eConf C0304052*, WG423 (2003), [hep-ph/0307032](#).